Article

Quantifying Raptors' Flight Behavior to Assess Collision Risk and Avoidance Behavior to Wind Turbines

Anne Cathrine Linder [1,*], Henriette Lyhne [2], Bjarke Laubek [3], Dan Bruhn [2,4] and Cino Pertoldi [2,5]

1   National Institute of Aquatic Resources, Technical University of Denmark, 2800 Kongens Lyngby, Denmark
2   Department of Chemistry and Bioscience, Aalborg University, 9220 Aalborg, Denmark
3   Vattenfall Renewable Wind DK A/S, 6000 Kolding, Denmark
4   Skagen Bird Observatory, 9990 Skagen, Denmark
5   Aalborg Zoo, 9000 Aalborg, Denmark
*   Correspondence: acali@aqua.dtu.dk

Abstract: Some wind farms have implemented automated camera-based monitoring systems, e.g., IdentiFlight to mitigate the impact of wind turbines on protected birds. These systems have promoted the collection of large amounts of unique data that can be used to describe flight behavior in a novel way. The aim of this study was to evaluate how this unique data can be used to create a robust quantitative behavioral analysis, that can be used to identify risk-prone flight behavior and avoidance behavior and thereby used to assess collision risk in the future. This was achieved through a case study at a wind farm on the Swedish island Gotland, where golden eagles (*Aquila chrysaetos*), white-tailed eagles (*Haliaeetus albicilla*), and red kites (*Milvus milvus*), were chosen as the bird species. These three species are generally rare breeds in Europe and have also been shown to be particularly vulnerable to collisions with wind turbines. The results demonstrate that data from the IdentiFlight system can be used to identify risk-prone flight behaviors, e.g., tortuous flight and foraging behavior. Moreover, it was found that these flight behaviors were affected by both weather conditions, but also their distance to the nearest wind turbine. This data can, thus, be used to evaluate collision risk and avoidance behavior. This study presents a promising framework for future research, demonstrating how data from camera-based monitoring systems can be utilized to quantitatively describe risk-prone behavior and thereby assess collision risk and avoidance behavior.

Keywords: IdentiFlight; avoidance response; golden eagle; white-tailed eagle; red kite; wind turbine curtailment; flight behavior; flight symmetry

1. Introduction

Wind energy production has undergone rapid development over the past decades, due to the increasing demand for green energy. This has in turn led to a green on green predicament, due to the adverse effects of turbines on many avian species [1–9]. These adverse effects of wind turbines on raptors result primarily from direct fatalities due to collisions and secondarily through habitat alteration and loss [9]. Loss et al. [7] estimated that bird fatality increases proportionally with increasing turbine height. The exact number of avian collisions with wind turbines is uncertain. Nonetheless, even relatively few fatalities can have detrimental effects on slow maturing species with low reproduction rates, e.g., raptors, especially when considering the cumulative effect of multiple wind farms. This is particularly an issue for species of conservation concern when considering regional and national populations [1,7]. Collision-related mortality is unevenly spread among species, with few species often accounting for a large proportion of collision victims [10]. Large soaring birds are known to be specifically vulnerable for collision with turbines [2,3,9,11]. Species-specific differences, such as differences in size and wingspan can contribute to some species groups being more prone to collisions with turbines. However, mortality cannot, as such, be compared across species, as some birds have a longer longevity, fewer nestlings,

and are generally rare. The loss of such individuals is worse, compared to common birds, e.g., the chiffchaff or mallard. In Europe, some birds have been described as vulnerable species, such as golden eagles (*Aquila chrysaetos*), white-tailed eagles (*Haliaeetus albicilla*), and red kites (*Milvus milvus*) [12].

Collision risk is assumed to be dependent on multiple factors, e.g., flight altitude, behavior, and morphology. In regard to flight behavior, some types of behavior, e.g., flying at altitudes within the turbine rotor zone and tortuous flight paths, have been described as more risk prone than others [6]. Another suggested predictor of collision risk is whether birds are migrating or engaging in local activities, e.g., foraging, as foraging individuals are expected to be less vigilant in regard to their flight direction and more focused on searching for prey on the ground [1,6,13,14]. Local individuals may also have a higher risk of collision, as they may have to move through the wind farm between their foraging grounds and nesting sites multiple times throughout a single day, and thus, possibly increasing their collision risk. Moreover, flight type is another behavioral factor suggested to affect collision risk. Large birds such as golden eagles, depend upon soaring flight to retain energy; however, this flight type may increase their risk of colliding with turbines, especially under less favorable conditions for gaining altitude [15–18]. Barrios and Rodríguez [15] found an increased collision rate when birds were forced to gain altitude using thermal soaring, i.e., slow circle-soaring flight on thermals, which often took place in airspace overlapping with turbines. Hence, flight type and collision risk are suggested to be affected by environmental factors such as weather (e.g., wind speed and direction, temperature, cloud coverage, and visibility) and topography [15,19]. Furthermore, the risk of collision is presumably also strongly affected by avoidance behavior [14].

Avoidance behavior is generally observed as changes in flight behavior and trajectories in response to wind turbines; this avoidance response can be found at different scales, i.e., micro-scale (last second) and meso-scale (within wind farm) avoidance responses to single turbines within a wind farm and macro-scale avoidance responses, avoiding the entire wind farm [18,20]. Garvin et al. [14] defined avoidance as changes in flight height or flight direction deviating away from turbines and found that raptors showing no response to turbines were individuals passing through the wind farm on a straight flight path. It has been suggested that raptors are more vulnerable to turbines due to lower avoidance compared to the avoidance of migratory species e.g., geese [21]. Dahl et al. [19] showed that white-tailed eagles displayed high risk flight behavior, i.e., no flight response and lack of avoidance close to turbines, which was also associated with high collision rates. However, multiple other studies have also found implications of raptors adjusting their flight trajectories to avoid wind turbines [22,23]. Whitfield and Madders [22] showed that red kites displayed avoidance rates of between 98 and 100%. These contradicting findings indicate that avoidance behavior is both site- and species-specific [3,14,24]. It is therefore necessary to gain an understanding of which variables affect flight behavior in general for specific species and sites to gain a more thorough understanding of avoidance behavior.

Regardless of avoidance behavior, some protected raptor species have been suggested to be more vulnerable to wind turbines; the impact of wind turbines on such species may, therefore, be mitigated by turbine curtailment [25]. Some wind farms, particularly in the United States, have implemented an automated camera-based monitoring system, e.g., IdentiFlight, to detect birds in flight and determine whether they are protected species, e.g., eagles. If a bird that is detected as one of the protected species has a calculated trajectory on course to a turbine or is within a specified radius of a wind turbine, the system will issue a curtailment recommendation resulting in curtailment of the wind turbine before a collision occurs [26]. However, the actual collision risk between raptors and wind turbines is presumably determined by the vigilance of individuals, i.e., their avoidance behavior, which is suggested to be dependent on multiple factors, e.g., weather conditions [8,14,19,20]. Knowledge of the avoidance behavior of protected raptors, such as eagles and the red kite, and how this behavior can be affected by environmental factors is therefore crucial to improving curtailment decisions. Curtailing wind turbines is expensive and energy

companies would, therefore, benefit from the development of behavior-specific curtailment models. Furthermore, the IdentiFlight camera system can provide a useful service to avian biologists, as it facilitates the collection of large amounts of data including not only flight trajectories based on spatial coordinates, but also images of individual birds throughout their flight trajectories, thus providing the unique opportunity of assessing flight behavior based on both flight trajectories and behavioral observations, i.e., flight orientation.

The development of camera-based monitoring systems at wind farms has enabled the collection of large amounts of data that can be used to describe the behavior of selected bird species, and thus, provides the possibility of creating quantitative behavioral analyses, which may be used to assess collision risk and avoidance behavior, potentially providing avian biologists with new imperative knowledge. Therefore, this study will investigate how the behavior of raptors can be quantified by using unique data from the IdentiFlight system, demonstrating how this type of data can be used to assess general flight behavior and investigate site and species-specific avoidance behavior. This was achieved in a case study investigating the behavior of golden eagles (*Aquila chrysaetos*), white-tailed eagles (*Haliaeetus albicilla*), and red kites (*Milvus milvus*) at a wind farm on the Swedish island Gotland.

It was a prerequisite that the flight behavior of these species could be described by flight altitude, flight type, active flight, and flight vigilance. It was expected that these variables describing flight behavior could be used to assess risk-prone behavior and thereby utilized as an indicator of collision risk. Flight behavior was also expected to be affected by weather variables, e.g., temperature, wind speed, and cloud coverage. Furthermore, it was expected that the birds' distance to the nearest turbine would impact their flight behavior, i.e., the individuals were expected to exhibit avoidance behavior. This proved that avoidance behavior could be detected through the new quantitative assessment of flight behavior in proximity to wind turbines.

2. Methods

2.1. Study Site

The study site is situated on Näsudden, a peninsula on Gotland's southwest coast. The terrain is generally flat and the highest peak of the island is only 135 m above sea level [27]. The peninsula is mainly covered by open fields, often utilized as foraging sites by the island's raptors. Gotland is home to breeding populations of approximately 55 pairs of golden eagles, 45 pairs of the white-tailed eagles and at least 15 pairs of red kites [28,29].

The island is not directly part of any migratory routes for these species and these species are, therefore, mainly represented by local individuals [30]. The wind farm consists of 55 turbines, ranging from 45–145 m in height. The first turbines were constructed in 1979. The observational area of the wind farm was defined by a radius of 400 m around the IdentiFlight (IDF) camera tower and included nine turbines (Figure 1). The remaining turbines on the wind farm were not covered by the IDF system, as a single IDF camera tower has a maximum range of one kilometer.

2.2. Data Collection

Observations of the selected species were collected using the IdentiFlight system over a period of 10 months in 2020, spanning from the middle of February to the end of November. Throughout this time period, the system was periodically out of operation and the study is therefore based on a total of 231 days over the course of the 10 months (Appendix A). These observations could include both local and non-local individuals of the three species; however, the majority of observations are expected to be local breeders. Out of the 231 days, raptors of the species golden eagle, white-tailed eagle or red kite were only observed within the observational area (up to 400 m away from the camera tower) of the wind farm on 153 of these days. During the study period, the IdentiFlight system only collected simulated curtailment data for the nine turbines; hence, the system was not actively curtailing turbines.

Figure 1. The IDF Tower (red drop) and the 400 m zone (orange circle) around the tower, i.e., the observational zone. The wind turbines that the birds within the 400 m zone flew closest to (orange crosses) and other turbines (grey crosses) within the wind farm.

2.2.1. IdentiFlight System

The IdentiFlight system was developed to detect eagles at risk of collision with a rotating wind turbine. The system can detect a bird that is up to one kilometer away from the camera tower and classify whether it is a protected species or not in real time. This species identification is based on IdentiFlight's machine vision algorithms that use a catalog of rules developed by pattern-recognition technology. Size, plumage, color, wing shapes and flight profiles are some of the variables used to classify birds. If a bird is identified as a protected species the system will then determine if a specific turbine or turbines should be shut down to prevent collision, based on a set of site-specific criteria (curtailment prescription) [26]. In the curtailment prescription, an outer and inner cylinder is determined for each turbine, based on the turbine height and rotor diameter. The system will issue a curtailment order resulting in the curtailment of a turbine if a bird, classified as a protected species, flies into the inner cylinder. If the bird flies between the outer and inner cylinder, the system will only issue a curtailment order if certain criteria are met, e.g., if the bird is flying toward a turbine with a flight speed of above a certain value. However, the system will never issue a curtailment order if the bird is flying outside of the outer cylinder (Appendix B.1).

The camera system consists of a ring of eight fixed wide-field-of-view cameras and a high resolution stereo camera mounted on top of a six-meter-high tower (Appendix B.2). The eight wide-field-of-view cameras use image sensor arrays to detect moving objects in the environment and begin to track them. These cameras collect 10 images per second and detect moving objects by comparing the placement of an object relative to the background between images. When a moving object is detected, the movable high resolution stereo camera is directed at the object and uses high magnification stereoscopic sensors to determine the distance to the object. Furthermore, the high resolution stereo camera collects approximately one image per second and gathers the necessary information to classify the object.

The IdentiFlight system provides a dataset with a large variety of variables, including bird images, describing each observation and providing each track with a unique Track ID (Appendix C). Furthermore, flight trajectories for each track are saved as Keyhole Markup Language (KML: a file format used to display geographic data) files, which can be imported into ArcGIS Pro [31]. Thus, a dataset with multiple observations of each track is produced, i.e., the flight trajectory of a bird's flight path illustrating its observed flight activity. Hereafter, when referring to observations, it is a reference to all observations (multiple observation for each track) and when referring to tracks, it is a reference to flight

trajectories, i.e., all observations summarized for each track. It should be noted that the automated data collection by the IdentiFlight system may be biased, as the tracks may be incomplete because the system may stop tracking birds for multiple reasons, one being the system identifying the target bird as not at risk of colliding with a turbine, e.g., due to the flight direction and position of the bird. The system also stops tracking birds if it mistakenly reclassifies the bird as a non-protected species, thus losing interest in the bird.

2.2.2. Weather Data

Temperature, wind speed and wind direction, provided by Vattenfall, were collected at 10 min intervals by weather stations on the turbines at a height of 80 m, portraying the weather conditions near the rotor zone of the turbines. Cloud coverage was measured at hourly intervals at a weather station in the southern part of Gotland, approximately 34 m above sea level. These data were downloaded from the Swedish Meteorological and Hydrological Institute [32].

2.3. Data Preparation

Observations from the collected data were filtered based on the species classified by the system in order to obtain a subset with the species golden eagle, white-tailed eagle, and red kite. The bird images were used to classify the head position of the raptors, as either oriented straight forward or down and whether or not the raptor was engaging in active flight (Figure 2). These classifications were performed for each observation. Only observations within 400 m of the camera system were used, as it was difficult to classify the head position for images taken at further distances. Furthermore, only tracks longer than 100 m were used, as shorter tracks were not considered to be fully descriptive of a bird's behavior within the area. This resulted in a dataset of 564 different tracks of the three selected species (Appendix D).

ArcGIS Pro [31] was used to analyze the flight trajectories (KML files). The flight trajectories were used to classify flight type, i.e., each track was assigned one of four different flight types based on a qualitative assessment of flight trajectories (Figure 3). The flight type straight describes raptors flying in a linear path with only minor directional deviations. Raptors flying in the same general direction, but with slightly larger directional deviations than those depicted as straight were classified as the flight type curvy. These two flight types presumably represent birds passing through the study site on route to another location, e.g., birds traveling from roosting sites to foraging sites. The flight type spiral represents raptors presumed to be using thermal soaring, i.e., soaring in updrafts using thermal convection; thus, directional changes were mainly in the same direction, creating loops while increasing altitude. When a raptor's flight path had no general flight direction and many large directional changes in all directions, the flight type was categorized as chaotic. This chaotic flight type may be attributed to local birds foraging within the study site.

The flight trajectories were also assessed by calculating the track symmetry and tortuosity, which was performed using the ArcPy package in Esri [31]. Track tortuosity was calculated for each track, as shown in Equation (1), where l_a is the actual track length and l_d is the direct track length, i.e., the shortest distance from a track's start point to the track's end point (Figure 4). This resulted in a measure of deviations from the most direct path, where a value of 1 represents a flight path with no deviations. The smaller the value, the more deviations from the direct flight path.

$$Tortuosity = \frac{l_d}{l_a} \tag{1}$$

Track symmetry was determined by calculating the angles of directional changes throughout the track. These angles ranged from $-180°$ to $180°$, distinguishing between left and right turns (Figure 5).

(**a**) Head oriented straight.

(**b**) Head oriented down.

(**c**) A series of images showing a bird in active flight, i.e., flapping its wings.

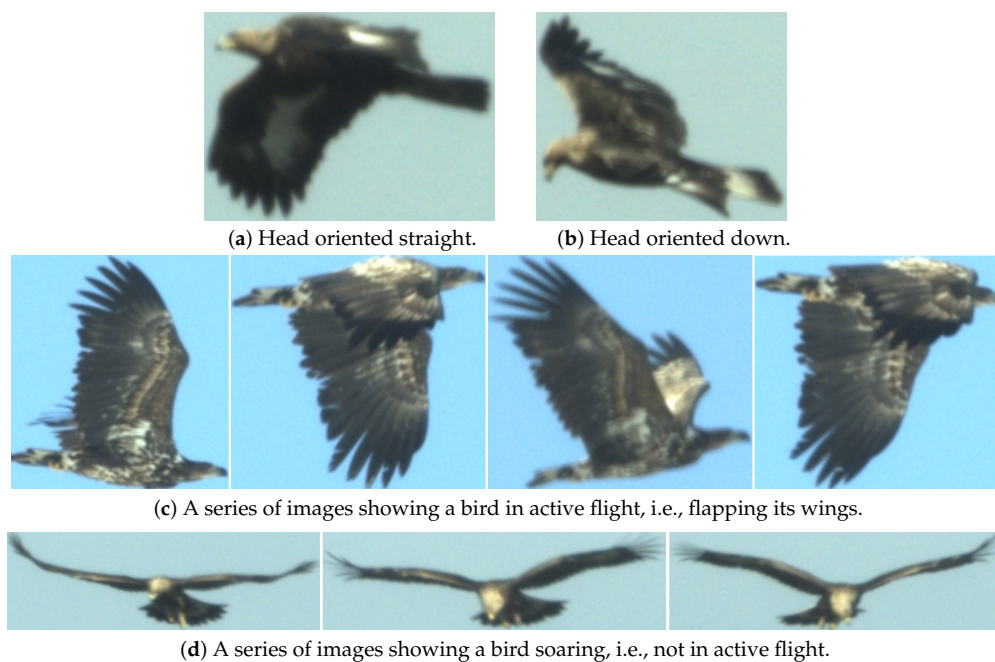(**d**) A series of images showing a bird soaring, i.e., not in active flight.

Figure 2. Examples of how behavior was scored based on bird images, a single image was used to classify head position and a series of images had to be used to classify active flight in order to evaluate wing movement between images.
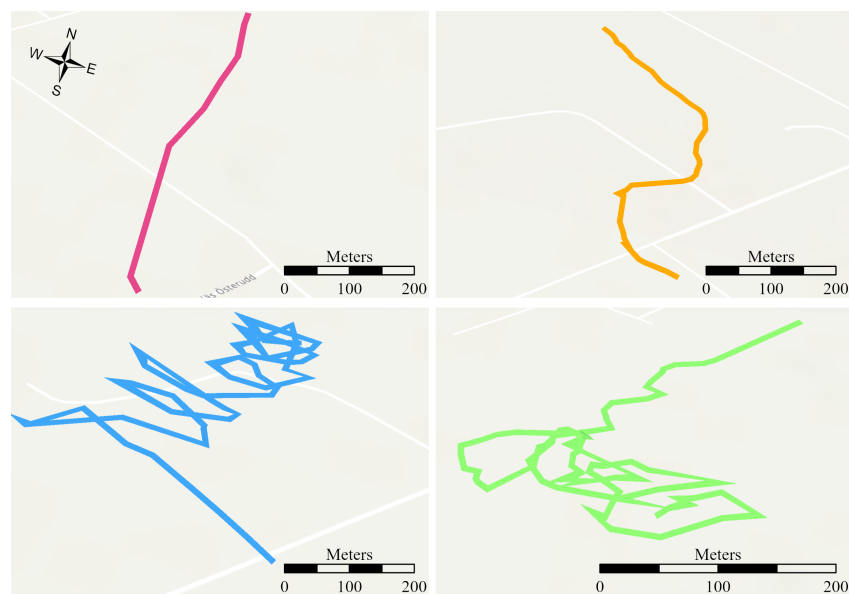

Figure 3. Examples of the four different track types: straight (pink), curvy (orange), spiral (blue), and chaotic (green). The images are based on three-dimensional tracks, i.e., multiple points with x, y, and z coordinates.
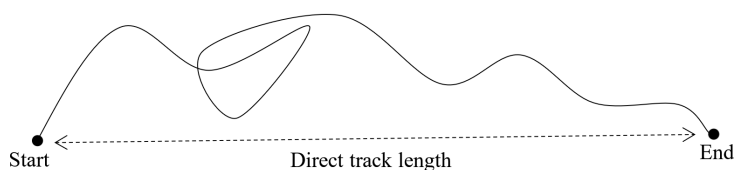

Figure 4. Model of a track, showing the direct track length (the dotted arrow) in comparison to the actual track length.
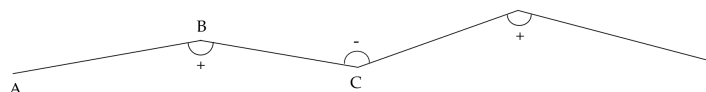
Figure 5. Model of a track. Right turns ranged from 0 to 180° and left turns from −180 to 0°, which are annotated with + and −, respectively. Trigonometry was used to calculate the angles; therefore, three points were used to calculate each angle, e.g., when calculating the angle for the point B, the points A and C were used as well.

To calculate the angles of the track, the inverse trigonometric function of cosine (arccos) was used as shown in Equation (2). A, B and C represent points, as shown in Figure 5, where AB is the distance from point A to point B, and BC is the distance between point B and C, and so on.

$$\angle B = arccos\left(\frac{AB^2 + BC^2 - AC^2}{2 \cdot AB \cdot BC}\right) \tag{2}$$

The signed track angles, i.e., directional changes were then summed for each track (Equation (3)). This resulted in a measure of flight symmetry, where a value of 0 represents a perfectly symmetrical track in terms of the number of turns and the size of them to the left and to the right. The larger the value, the more asymmetrical the track in relation to turns to either the left or the right.

$$Symmetry = \left|\sum_{i=1}^{n} \angle_i\right| \tag{3}$$

2.4. Data Analysis

The data analyses were carried out for all observations, but also for subsets of observations based on track type, flight type, flight direction, and flight altitude (Appendix D). For analyses involving flight vigilance or active flight, only individuals with more than three observations (bird images) were used. All tracks were divided into four subsets based on track type. Another subset was created that only included tracks with individuals engaging in active flight. All observations were divided into two subsets based on flight direction, i.e., flying towards the wind turbine or away from the wind turbine; this was based on whether the distance to the nearest turbine was decreasing or increasing, meaning that most individuals are present in both subsets, as throughout their track they fly both towards and away from a turbine. Furthermore, three subsets were created by dividing observations based on flight altitude into the following categories: below, in or above the rotor zone of the nearest turbine, i.e., each individual could be represented in multiple subsets (see Appendix B.1 for rotor zone definitions). The statistical analyses were conducted in R version 4.1.1 [33].

2.4.1. Flight Behavior Classifications

To assess how the general flight behavior of raptors can be quantified and how it is affected by the weather, associations among the different variables describing flight behavior and between these variables and weather variables were tested with Spearman's rank correlations (r_s) [34] (Table 1). Bonferroni's correction for multiple comparisons was applied, as the same variables are included in multiple tests [34]. Furthermore, to evaluate the applicability of track symmetry and track tortuosity, as indicators of the overall track type, a box plot of each variable was created, describing the median and interquartile range (25–75%) for each track type. To assess the respective univariate relationships between different response variables describing flight behavior (% time spent looking down, flight altitude, track symmetry and track tortuosity) and various explanatory weather variables (temperature, wind speed and cloud coverage), correlation coefficients were calculated and

the relationships between these variables were visualized with linear regressions. The univariate relationships between the aforementioned variables describing flight behavior were also visualized with linear regression and their respective correlation coefficients were calculated as well. All regressions were based on grouped medians of the dependent variable, that were determined by class intervals of independent variables, with horizontal bars representing the interquartile range (IQR) to illustrate the variation around the medians. This was performed for all subsets.

Table 1. Overview of all univariate tests, with Spearman's rank correlation being annotated by r_s.

	Response Variable			
Independent Variable	**Flight Vigilance**	**Flight Altitude**	**Track Symmetry**	**Track Tortuosity**
Flight vigilance			r_s	r_s
Active flight	r_s		r_s	r_s
Flight altitude	r_s		r_s	r_s
Track symmetry	r_s			
Track tortuosity	r_s			
Turbine distance	r_s	r_s	r_s	r_s
Cloud coverage	r_s	r_s	r_s	r_s
Temperature	r_s	r_s	r_s	r_s
Wind speed	r_s	r_s	r_s	r_s

2.4.2. Avoidance Behavior

To assess avoidance behavior, i.e., behavioral changes, such as changes in flight altitude, in proximity to wind turbines, flight altitude was assessed as the response variable in relation to distance to nearest turbine as the explanatory variable. This was achieved by calculating the correlation coefficient and the relationship was also visualized with a linear regression based on grouped medians. This was also repeated for all subsets. It was assumed that avoidance behavior would only be observed within a certain radius of a wind turbine. Therefore, the cumulative regression between distance to nearest turbine and flight altitude was calculated with increasing turbine distance, to find the distance at which the relationship weakened. This distance was then used as an upper limit for the analysis of avoidance behavior. This was repeated for all subsets.

2.4.3. Collision Risk

In an attempt to quantify collision risk, generalized linear models were created to determine which variables affect flight behaviors influencing collision risk, i.e., flight vigilance, flight altitude, track tortuosity, and track symmetry. To assess collinearity between explanatory variables, Spearman's correlation coefficient (r_s) was calculated among the covariates and pairwise scatter-plots were created to detect obvious correlations among the covariates (Appendix E). The possible explanatory variables included distance to nearest turbine, wind speed, cloud coverage, and temperature, but depended on the flight behavior being assessed; the other flight behaviors were also often included as possible explanatory variables. Automated model selection (glmulti) was then used to find the best regression model based on the prediction error using the Akaike information criterion (AIC). The automated model selection builds all possible unique models from a list of explanatory variables, i.e., all models are compared (it is not iterative) [35]. The automated model selection was carried out for models both with and without pairwise interactions and the final models were then selected using an ANOVA χ^2 test comparing the models with and without interactions [36].

3. Results

3.1. Flight Behavior Classification

There was a difference in track symmetry and track tortuosity between the different track types (Appendix F.1). Moreover, flight altitude was negatively correlated with wind speed ($r_s = -0.370$ ***) and raptors flew at lower altitudes with increasing wind speeds (Figure 6). When assessing this correlation for each track type individually, this association was strongest for individuals flying in curvy patterns ($r_s = -0.470$ ***). There was also a correlation between flight altitude and cloud coverage ($r_s = 0.0349$ **) and between flight altitude and temperature ($r_s = 0.0833$ ***; however, these correlations were weaker than that of wind speed (Appendix F.2).

There was a significant positive correlation ($r_s = 0.309$ ***) between general flight vigilance (time spent looking down) and track asymmetry (sum of directional changes) (Appendix F.3). The more asymmetrical a raptor's flight path was, the less vigilant they were. Furthermore, for individuals in active flight, the relationship between general flight vigilance and flight asymmetry was more positively correlated ($r_s = 0.426$ ***) (Appendix F.4). General flight vigilance was negatively correlated ($r_s = -0.310$ ***) with track tortuosity, indicating that raptors with more direct paths also were the most vigilant in their flight direction (Appendix F.3). General flight vigilance was also negatively correlated ($r_s = -0.427$ ***) with time spent on active flight, meaning that raptors actively flying were more vigilant in their flight direction (Appendix F.3). There was also a significant positive correlation between general flight vigilance and flight altitude ($r_s = 0.135$ ***). However, when looking at this relationship for each track type individually, only straight tracks also showed a significant positive correlation ($r_s = 0.208$ ***). For chaotic tracks, this correlation was negative ($r_s = -0.149$ *) and no significant correlation occurred for the two other track types (Appendix F.5).

3.2. Avoidance Behavior

There was a weak correlation between distance to nearest turbine and flight altitude for all track types ($r_s = 0.0658$ ***) (Appendix F.6). When grouping the tracks by type, a slightly larger positive correlation occurred for the track types curvy ($r_s = 0.110$ ***), and spiral ($r_s = 0.134$ ***), whereas for chaotic tracks this correlation was negative ($r_s = -0.0854$ **) and for straight tracks this correlation was not significant ($p > 0.05$).

Moreover, there was a significant positive correlation between distance to the nearest turbine and flight altitude when raptors were flying towards the nearest turbine ($r_s = 0.158$ ***) and the correlation was slightly stronger when raptors were flying away from the nearest turbine ($r_s = 0.209$ ***) (Figure 7). When raptors were flying towards a turbine, there was a positive correlation between distance to nearest turbine and flight vigilance for all three altitude zones separately (above: $r_s = 0.126$ ***; below: $r_s = 0.147$ ***; in: $r_s = 0.0789$ *) (Figure 8).
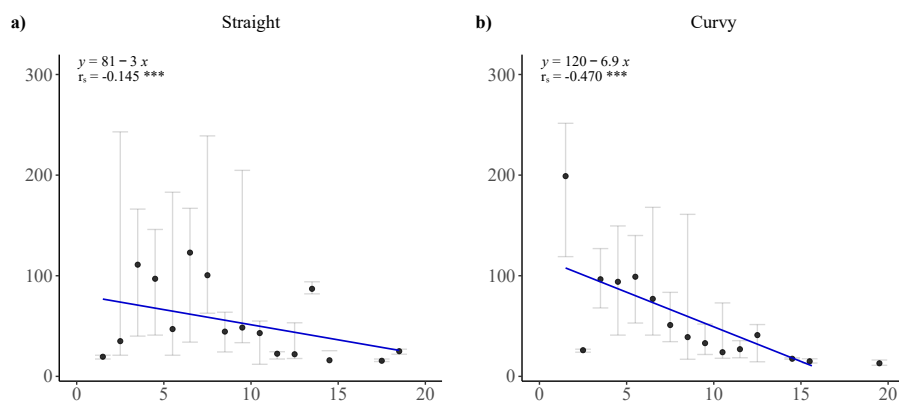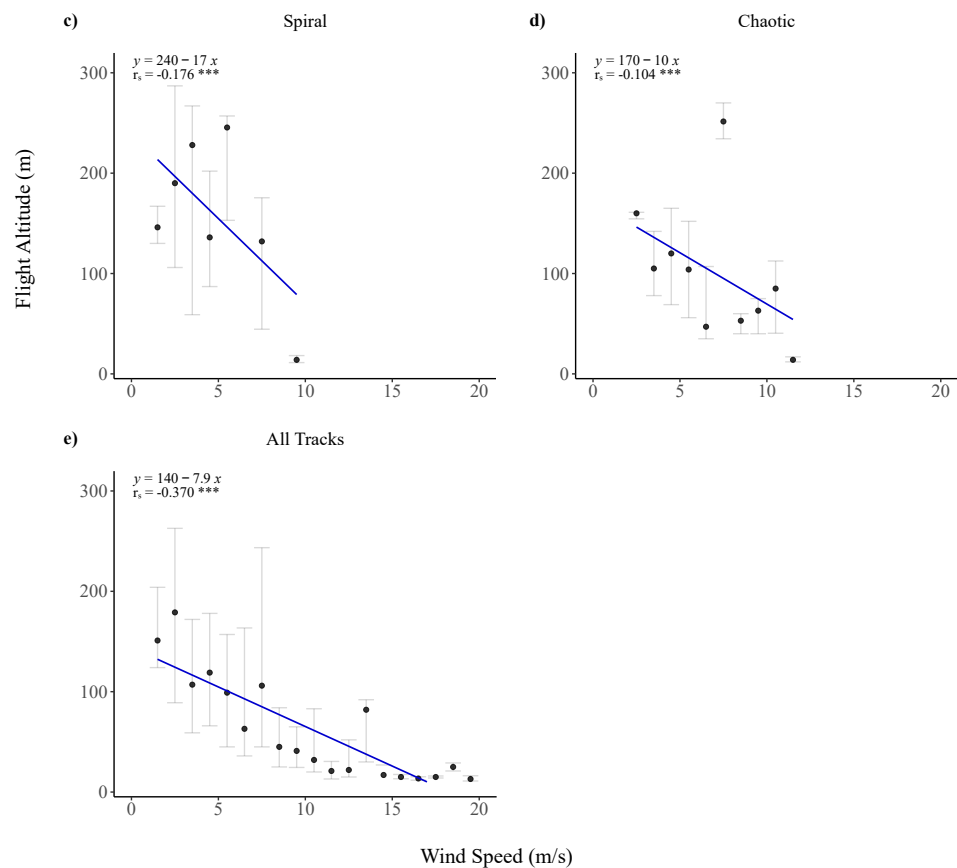

Figure 6. *Cont.*

Figure 6. Linear regression of flight altitude above ground level in relation to wind speed, (**a–d**) grouped by track type and for (**e**) all track types collectively. For each regression, the median flight altitude was used for wind speed at each m/s. The regression equation and correlation coefficient (r_s, *** $p < 0.001$) is given for each plot. The horizontal bars represent the variance around each median (IQR).
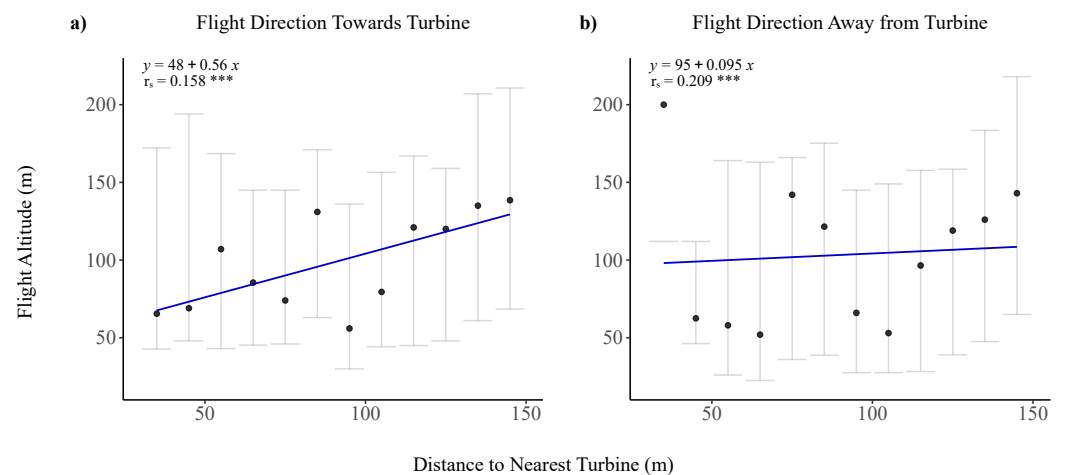

Figure 7. Linear regression of distance to the nearest turbine (<150 m) in relation to flight altitude above ground level grouped by flight direction (**a**) flying towards the nearest turbine and (**b**) flying away from the nearest turbine. For each regression, the median flight altitude (m) was used for every 10 m. The regression equation and correlation coefficient (r_s, *** $p < 0.001$) is given for each plot. The horizontal bars represent the variance around each median (IQR).
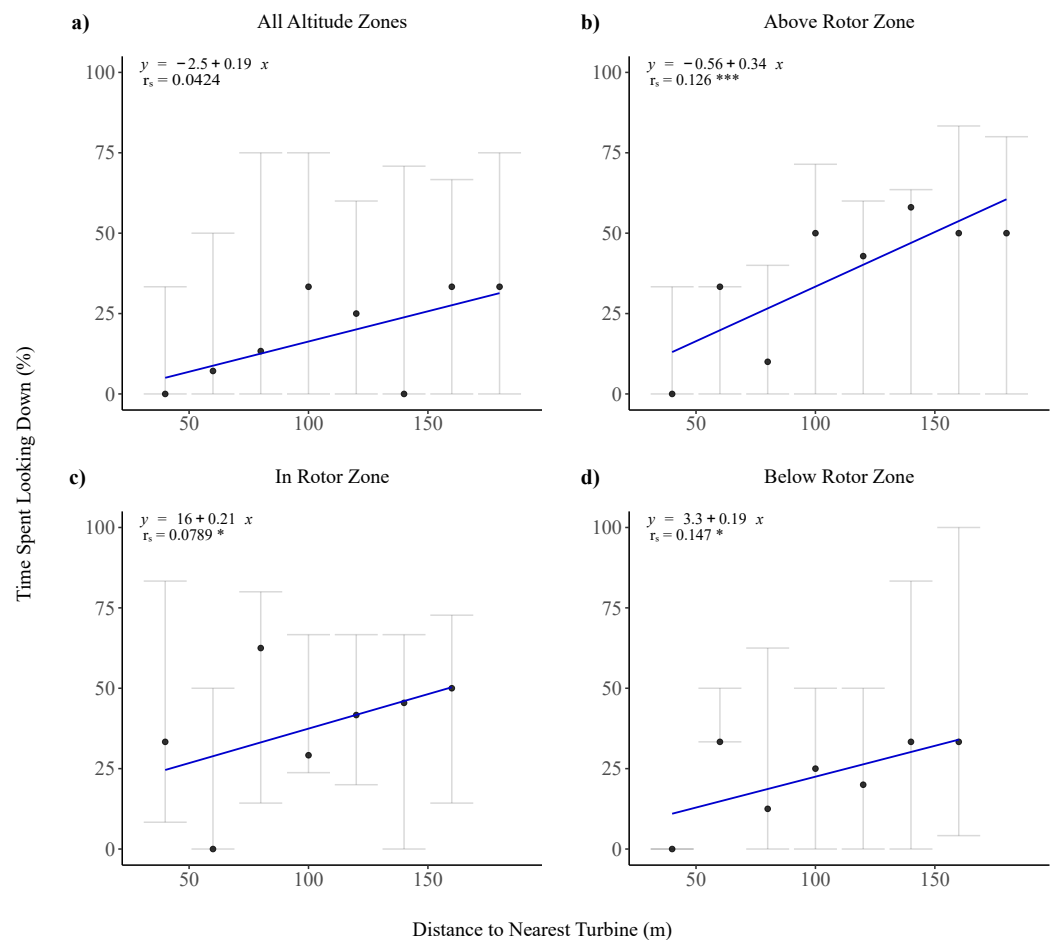
Figure 8. Linear regression, for individuals flying towards a turbine, of the proportion of time the birds spent looking down for each track (median values for turbine distance groups per 20 m) in relation to distance of the nearest turbine for (**a**) all individuals, (**b**) individuals flying above rotor zone, (**c**) individuals flying in rotor zone, and (**d**) individuals flying below rotor zone. The regression equation and correlation coefficient (r_s, * $p < 0.05$, *** $p < 0.001$) is given for each plot. The horizontal bars represent the variance around each median (IQR).

3.3. Collision Risk

The comparison of models with and without interactions indicated the simpler of the two models, i.e., the model without interactions, to be the better choice when assessing track tortuosity as the response variable, as adding interaction terms did not significantly improve the model. When assessing the other response variables, i.e., flight vigilance, flight altitude, and track symmetry, respectively, the addition of interaction terms significantly improved the model's goodness of fit (Appendix G).

When assessing flight vigilance as the response variable, the automated model selection indicated that flight altitude (evidence weight = 1.00) and track tortuosity (evidence weight = 0.999) were the two most important model terms (Figure 9a). However, all covariates, with the exception of turbine distance, significantly contributed to explaining the variation of flight vigilance. The automated model selection for assessing flight altitude, as the response variable, indicated that flight vigilance (evidence weight = 1.00) and temperature (evidence weight = 1.00) were the two most important model terms; however, all other covariates also significantly contributed to explaining the variation in flight altitude (Figure 9b). When assessing the response variable track tortuosity, the evidence highlighted active flight (evidence weight = 0.996) and flight vigilance (evidence weight = 0.910) as the only covariates significantly contributing to the variation in track tortuosity (Figure 9c). When assessing track symmetry as the response variable, flight altitude was included in

three out of the four model terms with an evidence weight of over the threshold of 0.8 (Figure 9d). It should be emphasized that the absolute results from the automated model selections should only be interpreted as indications and should not be taken literally.
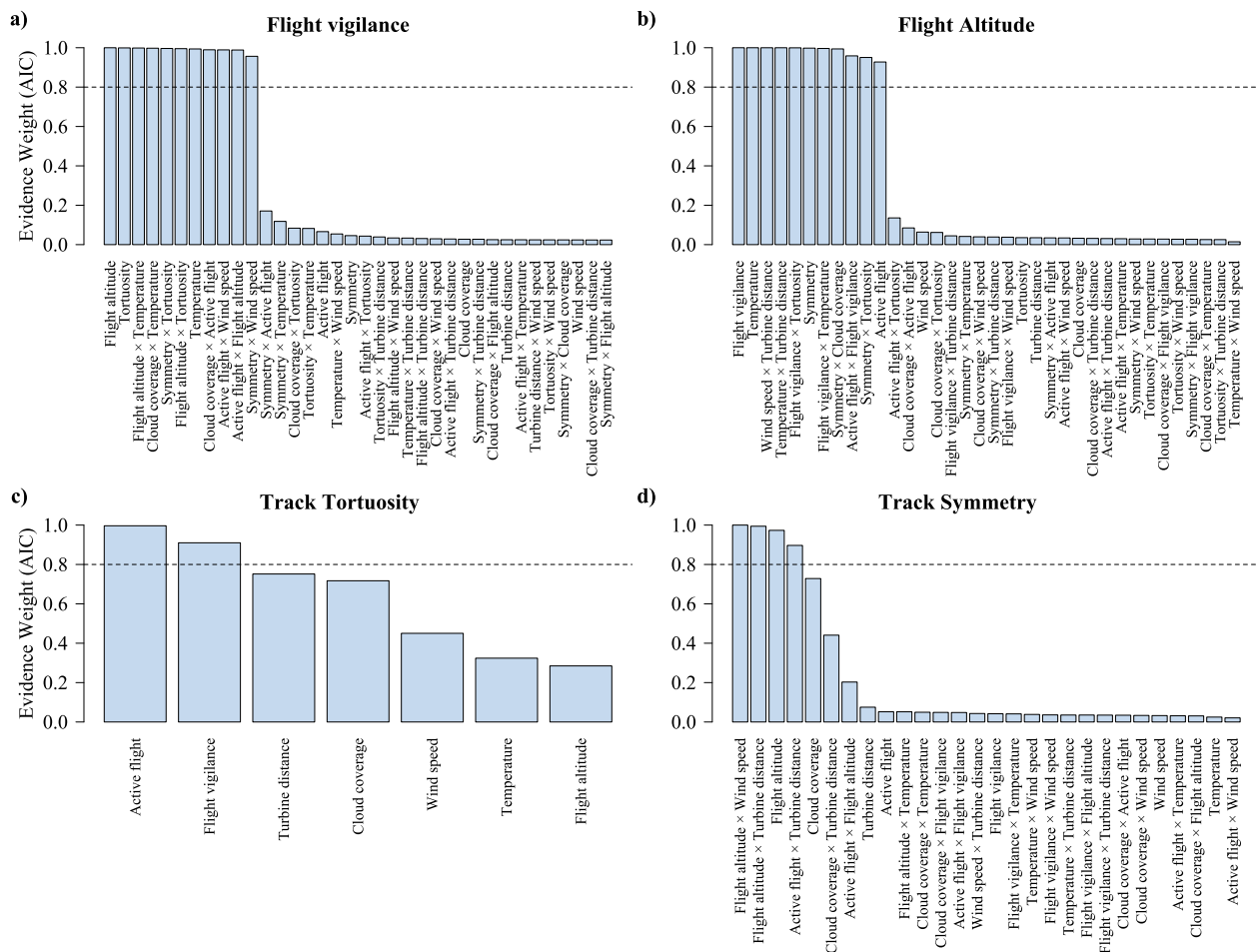

Figure 9. Relative importance of each model term when assessing (**a**) flight vigilance as the response variable with interactions, (**b**) flight altitude as the response variable with interactions, (**c**) track tortuosity as the response variable without interactions, and (**d**) track symmetry as the response variable with interactions. Each term's relative importance was estimated with the automated model selection as the sum of Akaike evidence weights of all models in which the term appears.

4. Discussion

The negative effects of wind turbines on birds result primarily from collision-related fatalities and secondarily through displacement effects resulting in habitat loss [9,37]. The precise number of collision-related fatalities is uncertain. Nonetheless, large soaring raptors are known to be specifically vulnerable for collision with turbines [2,3,9,11]. Furthermore, some wind farms are located close to the nesting sites of these species; thus, the risk of wind farms having a significant impact on both local and migrating raptors is likely high. Such a negative impact can have detrimental effects on slow-maturing species with low reproduction rates, particularly for species of conservation concern when considering regional and national populations [1,7]. This research provides an important step in understanding the effects of wind farms on raptors.

4.1. Flight Behavior as a Predictor of Collision Risk

The results of the case study demonstrate how flight trajectories can be used to describe flight behavior by classifying track type. Moreover, track symmetry and tortuosity can be used to quantitatively assess risk-prone behavior. Previous studies have often described tortuosity as an indicator for collision risk, indicating birds with a more tortuous flight path to be at higher risk for collision [6,38,39]. The inference of these studies is based on the expectation that a more tortuous flight path is associated with a larger amount of time flying; during flight, there will always be a collision risk. Furthermore, the associations between flight vigilance and flight tortuosity, respectively, found in this study, indicate that individuals with a more tortuous flight behavior are less vigilant, hence supporting the hypothesis that birds with a tortuous flight path are at increased risk for collision. This is further supported by the multivariate analysis, which also indicated track tortuosity to be an important model term when assessing flight vigilance as the response variable. Moreover, this analysis also indicates flight altitude to be the most important model term in this analysis, i.e., flight altitude was the covariate contributing the most to explaining the variation in flight vigilance. This corresponds to previous studies suggesting flight altitude in relation to the rotor zone to be an important predictor of collision risk, i.e., flight in the rotor zone is associated with a higher collision risk [6,14,38–40]. Flight altitude has previously been found to be determined by movement type, e.g., migratory or local movement [6]. Katzner et al. [6] and Bergen et al. [39] found that migratory birds flying in a linear fashion flew at higher altitudes. Contrary to this, the results in this study found individuals flying at higher altitudes to have more asymmetric tracks. These contradicting results are, however, likely to be due to the raptors on Gotland mainly consisting of breeding populations, as the island is not directly part of any migratory routes for these species [30]. The raptors in this study are therefore assumed to be mainly local birds; however, some of the studied raptors may be migratory. However, other factors, such as, weather conditions and distance to nearest wind turbine may further explain this behavior. Similar to the findings in this study, Dahl et al. [19] found that occurrences below the rotor zone were mainly individuals engaging in directional flight and some engaging in social behavior.

Effect of Weather on Flight Behavior

Understanding how weather affects flight behavior is important for developing risk-assessment models. The multivariate analysis indicated that all three weather variables contribute to explaining flight behavior. Moreover, the univariate analysis indicated that raptors flew at lower altitudes with increasing wind speeds. In accordance with these findings, previous studies also found that eagles were more likely to fly at altitudes under 150 m at higher wind speeds [40,41]. Kuehn et al. [40] suggests that these results reflect an increasing collision risk at higher wind speeds. Contrary to this, we suggest that while moderate wind speeds (5–10 m/s) result in an increased collision risk, due to the resulting flight altitudes being within the rotor zone, high wind speeds (>10 m/s) generally result in flight altitudes below the rotor zone and the risk of collision with moving rotor blades is therefore negligible.

4.2. Avoidance Behavior

The findings of the case study prove the use of variables describing flight behavior and thereby camera-based monitoring systems such as IdentiFlight for evaluating avoidance behavior, as the results indicate that golden eagles, white-tailed eagles and red kites exhibit some degree of meso-avoidance to the turbines within the wind farm on Gotland. However, the correlations describing avoidance behavior are generally weak, and should, therefore, only be interpreted as general indications. These weak correlations may be due to avoidance behavior being highly species-specific [3].

Moreover, previous studies show that raptors exhibit avoidance behavior by increasing flight altitude in proximity to turbines [8,14,16,20,23]. In this study the raptors studied decreased flight altitude in proximity to turbines. This response is also an indication

of avoidance behavior, as it can be argued that avoidance also can take place under the rotor zone. This avoidance response became more evident when dividing the track types according to flight direction. This avoidance response may be explained as when nearing a turbine the use various flight methods to increase altitude is reduced.

Furthermore, when comparing the avoidance behavior of individuals oriented towards the nearest turbine when flying either above, below or in the rotor zone, a positive correlation was found between distance to nearest turbine and time spent looking down for all three altitude zones. While this correlation was largely similar for individuals flying at altitudes above or below the rotor zone, the correlation was weaker for individuals flying towards the turbine at altitudes within the rotor zone. This could indicate that individuals flying at altitudes within the rotor zone exhibit a lower avoidance behavior and are at a larger risk for colliding with the turbine. Similarly, Garvin et al. [14] found the individuals flying in close proximity to the turbines generally demonstrated high risk behaviors, displaying no signs of avoidance.

5. Conclusions

This study provides a framework for future research, using data from camera-based monitoring systems, demonstrating how flight trajectories and bird images can be utilized to describe risk prone behavior and thereby assess collision risk and avoidance behavior. Thus, providing a crucial step towards quantifying collision risk in future predictive models. However, this study is only based on assumptions that behaviors decreasing flight vigilance, e.g., foraging, and tortuous flight are more prone to collision. It is, therefore, necessary to assess the behavior of individuals hit by turbines prior to the collision. The use of camera-based monitoring systems along with a collision-detecting system such as the WT-Bird system, that can detect collisions through the use of acoustic sensors on turbine blades [42] would enable the necessary data to be collected. Future studies should also focus on the foraging behavior of birds and should more specifically investigate the effect of carrion located under the rotor. This could be achieved by eliminating carrion under the rotors of the wind turbines and comparing the raptors' flight behavior in the two different situations, with and without carrion. This study provides a quantitative method that can be utilized to analyze such data and factually determine which behaviors lead to an increased collision risk.

Author Contributions: Conceptualization, A.C.L., B.L., C.P., D.B. and H.L.; methodology, A.C.L.,B.L., C.P., D.B. and H.L.; formal analysis, A.C.L.; investigation, A.C.L. and H.L.; resources, B.L.; data curation, A.C.L. and H.L.; writing—original draft preparation, A.C.L.; writing—review and editing, A.C.L., B.L., C.P. and D.B.; visualization, A.C.L.; supervision, B.L., C.P. and D.B. All authors have read and agreed to the published version of the manuscript.

Data Availability Statement: The data presented in this study are available on request from the corresponding author.

Conflicts of Interest: The authors declare no conflict of interest.

Appendix A. Operational Days

Table A1. Number of days where the camera system were operational, number of days with sightings of the selected raptor species (red kite, golden eagle, and white-tailed eagle), and number of tracks for each month.

Month	Operational Days	Days with Raptors	Number of Tracks
February	20	14	53
March	31	25	153
April	30	23	91
May	31	20	69
June	12	8	8
July	11	6	20
August	18	16	87
September	30	23	140
October	26	13	39
November	22	5	12
Total	231	153	672

Appendix B. IdentiFlight System

Appendix B.1. Curtailment Prescription

Table A2. Model type, number of turbines, rotor diameter, hub height, rotor zone, radius of outer and inner cylinder, and height of outer and inner cylinder for covered and partially covered wind turbines.

| Model	Number of Turbines	Rotor Diameter (m)	Hub Height (m)	Rotor Zone (m above Ground)	Radius Outer Cylinder (m)	Radius Inner Cylinder (m)	Height Outer Cylinder (m)	Height Inner Cylinder (m)
Covered								
Vestas V27	1	27	31	15.5–46.5	700	250	300	200
Vestas V29	1	29	31	14.5–47.5	700	250	300	200
Vestas V90	1	90	80	33.0–127	700	400	400	250
Partially covered								
Kenersys K100	1	100	85	33.0–137	600	300	400	250
Vestas V47	2	47	45	19.5–70.5	600	300	300	200
Vestas V90	2	90	80	33.0–127	700	300	400	250
Vestas V100	1	95	100	50.5–149.5	700	400	400	250
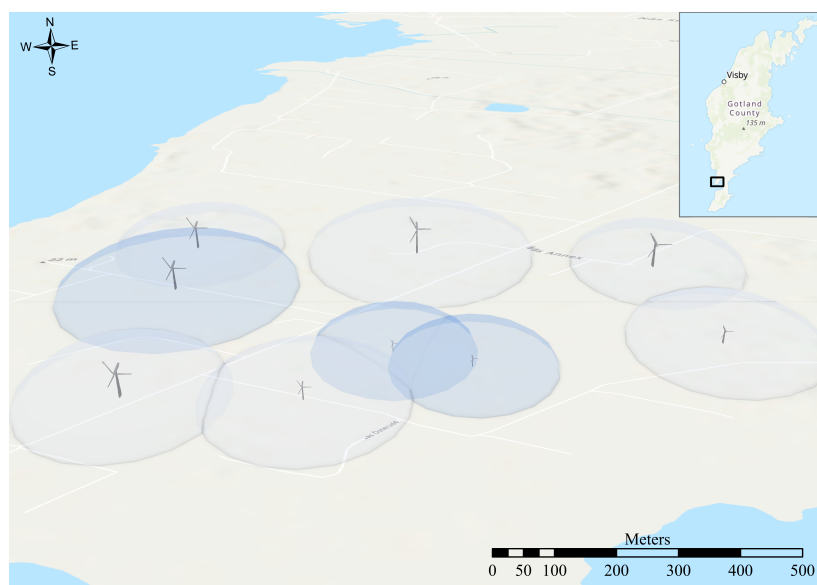
Figure A1. Fully covered (dark blue) and partially covered (light blue) wind turbines by the IDF tower. The horizontal curtailment zone (radius of inner cylinder) is shown around each turbine.

Appendix B.2. IdentiFlight Camera System

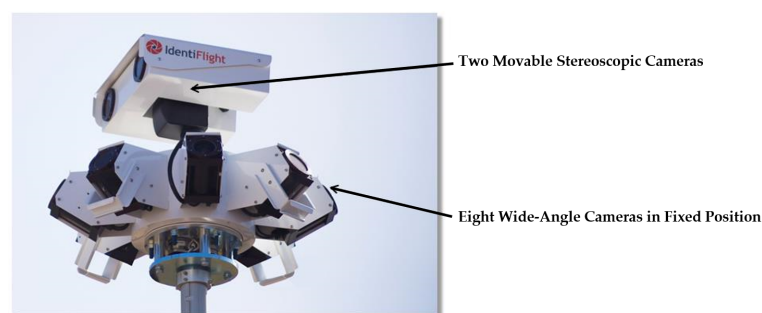

Figure A2. IdentiFlight tower at study site.

Figure A3. Imaging head components of the IdentiFlight tower. The bottom part consist of eight fixed cameras that can detect eagle sized objects and separate important from unimportant motion of birds. When important motion is detected, the top part tracks that bird as it consist of two movable cameras that also measure the distance of the the bird it is tracking.

Appendix C. IdentiFlight Data

The IDF system registers a large variety of variables for each observation of each track (Figure A4). Whenever a bird of interest is detected, it is assigned a unique track ID that is used for all observations of that bird. For each observation, an image is taken of the bird at that specific time, as the system notes the time and date. Furthermore, the longitude and latitude as well as the height above ground level is registered, which gives multiple

coordinates of each bird, i.e., tracks. The horizontal distance between the bird and camera tower as well as the distance between the bird and nearest turbine are also registered for each observation. Moreover, the system determines the species of each bird and gives a confidence level of the species classification. The system can classify a bird in the following categories: eagle, white-tailed eagle, golden eagle, non eagle, red kite, red or black kite, buzzard, gull, and other avian species.

Figure A4. Example of data output given by the IdentiFlight system.

Appendix D. Subsets

Table A3. Number of observations and tracks for each dataset and each subset based on track type, distance to turbine and altitude zone, respectively. For analyses containing all tracks and the variables, % time looking down and active flight, the dataset ≥100 m & ≥4 images was used. Otherwise the dataset the ≥100 m was used for analyses with all tracks. Tracks with odd deviations were removed from all datasets. For the subset dividing observations by altitude zone only observations within 180 m of the nearest turbine were used.

	Observations	Tracks
All tracks		
≥100 m	8036	564
≥100 m & ≥4 images	7796	442
Divided by track type		
Straight	1418	130
Curvy	3190	200
Spiral	1892	60
Chaotic	1296	52
Divided by altitude zone		
Above rotor zone	1311	256
Below rotor zone	820	236
In rotor zone	1580	320

Appendix E. Testing for Collinearity

To assess collinearity Spearman's correlation coefficient was calculated among the covariates and pairwise scatter-plots were created to detect obvious correlations among the covariates.
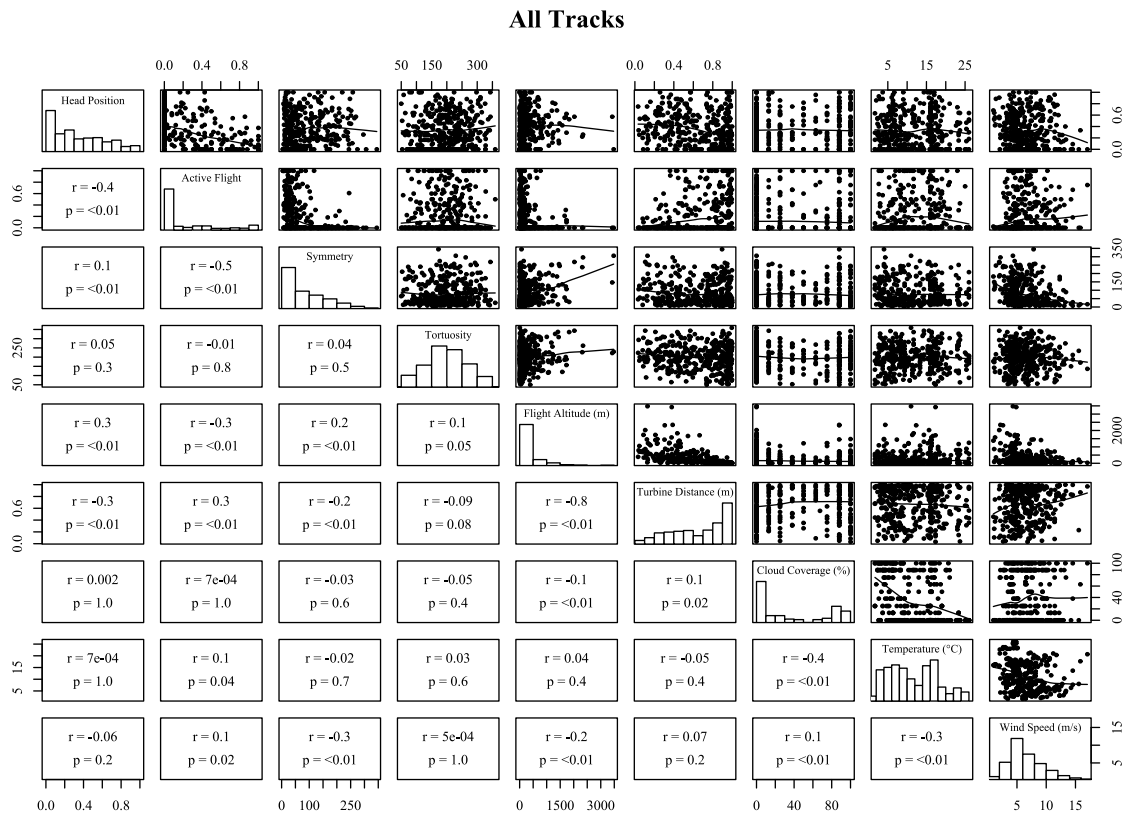
All Tracks

Figure A5. Correlation between the different continuous predictor variables.

Appendix F. Supplementary Results

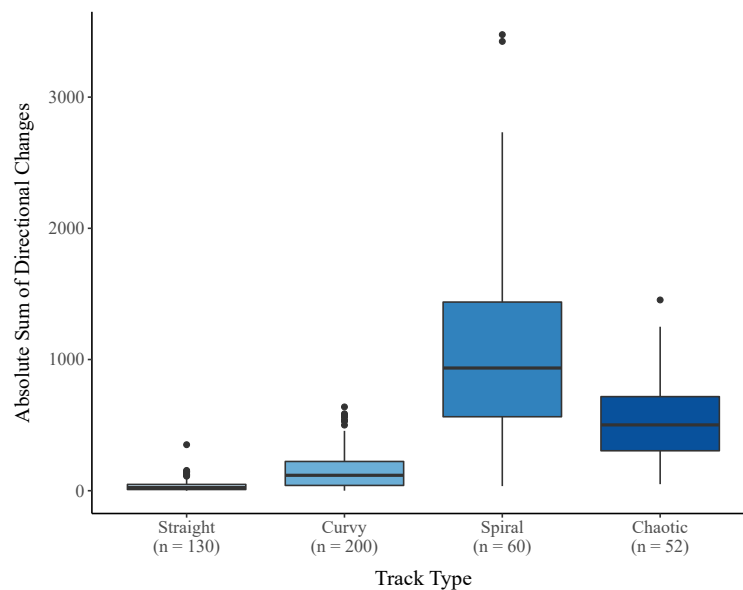*Appendix F.1. Flight Behavior Classification*

Figure A6. Track symmetry quantified by the absolute sum of directional changes (measured as angles) grouped by track type. Note that the larger the value the more asymmetrical the track is. The number of tracks each subset is based on is annotated under each track type.
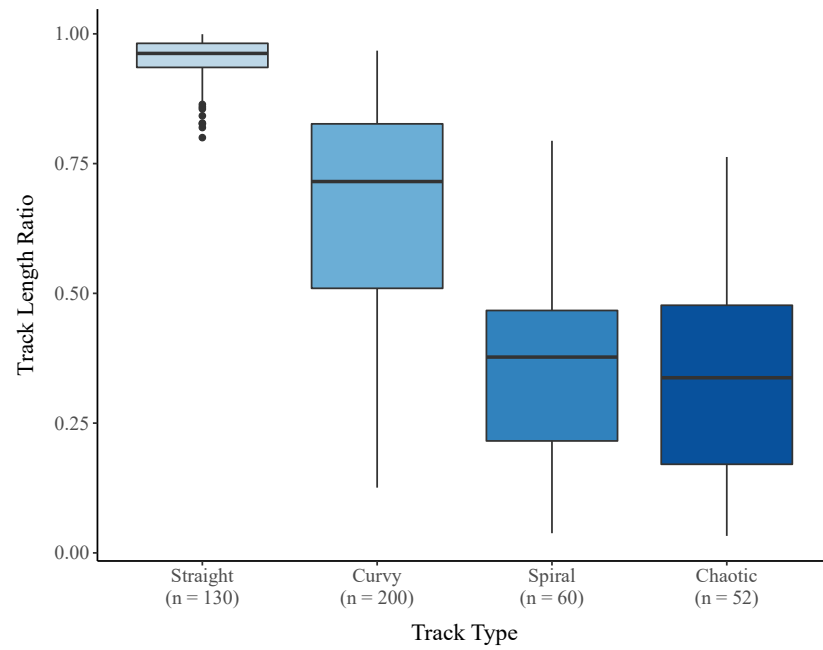
Figure A7. The ratio between the shortest path from a track's start to end point and the actual track length, grouped by track type. The number of tracks each subset is based on is annotated under each track type.

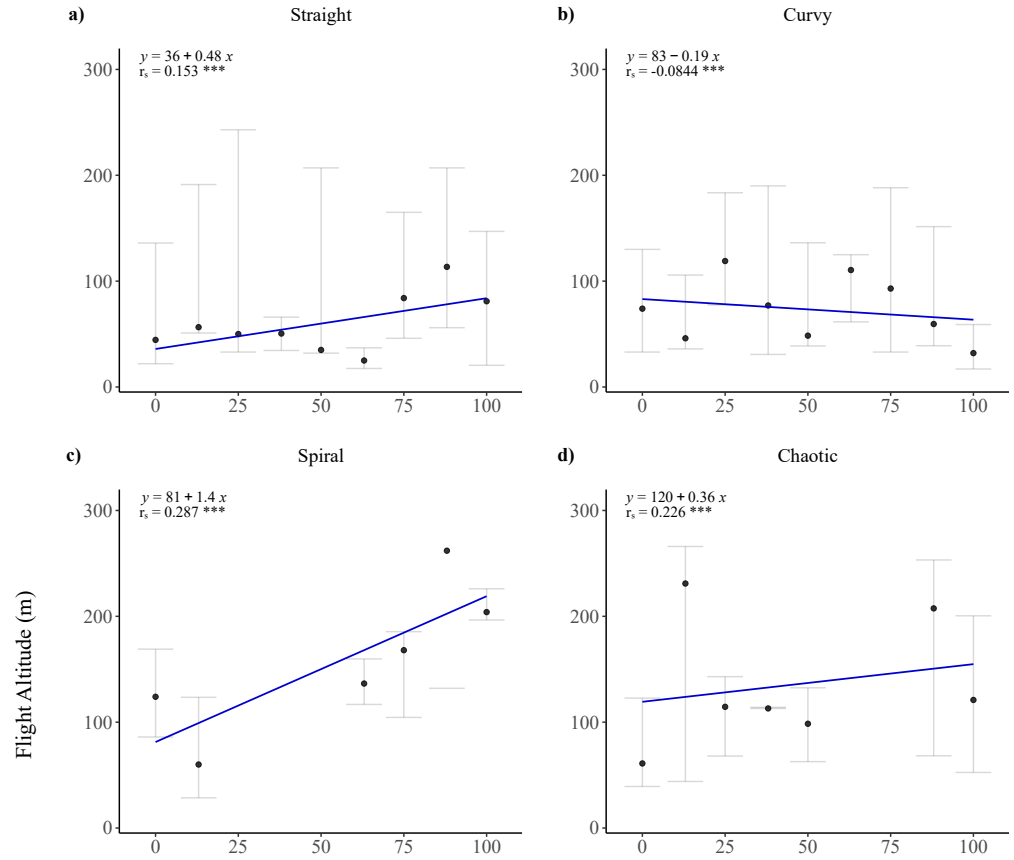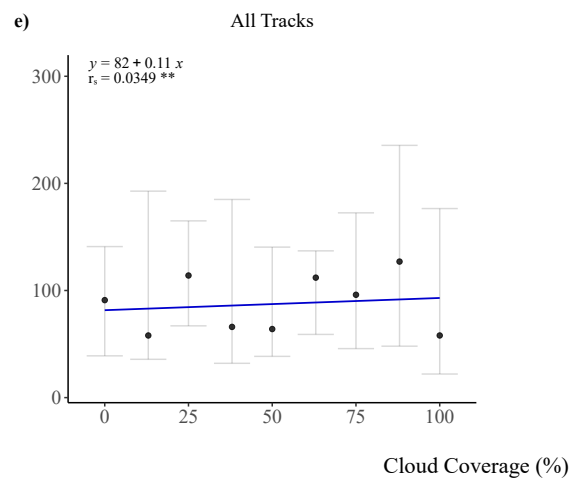*Appendix F.2. Flight Altitude in Relation to Weather*

Figure A8. *Cont.*

e) All Tracks

$y = 82 + 0.11 x$
$r_s = 0.0349$ **

Figure A8. Linear regression of flight altitude above ground level in relation to cloud coverage, (**a**–**d**) grouped by track type and for (**e**) all track types collectively. For each regression, the median flight altitude was used for each % cloud coverage. The regression equation and correlation coefficient (r_s, ** $p < 0.01$, *** $p < 0.001$) is given for each plot. The horizontal bars represent the variance around each median (IQR).
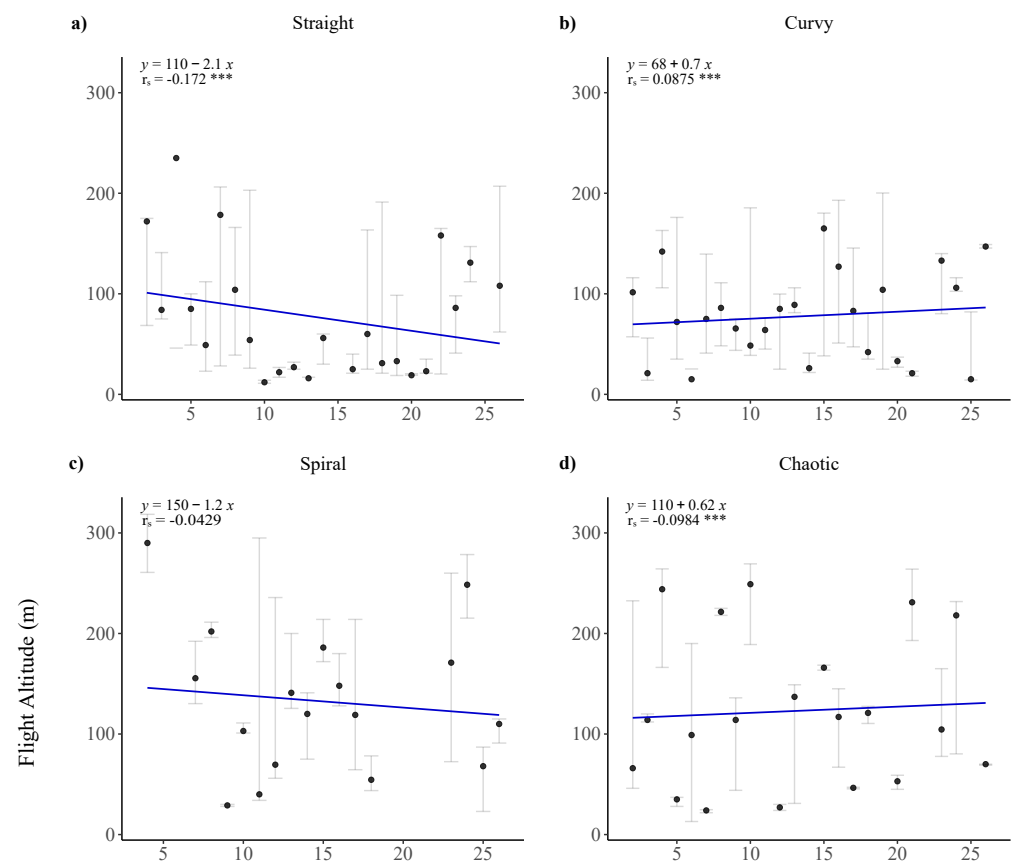
a) Straight

$y = 110 - 2.1 x$
$r_s = -0.172$ ***

b) Curvy

$y = 68 + 0.7 x$
$r_s = 0.0875$ ***

c) Spiral

$y = 150 - 1.2 x$
$r_s = -0.0429$

d) Chaotic

$y = 110 + 0.62 x$
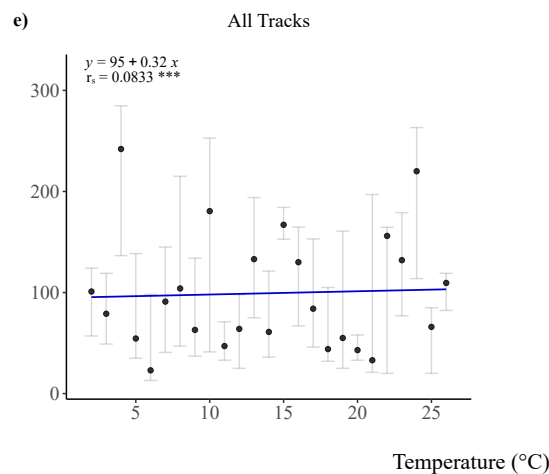$r_s = -0.0984$ ***

Figure A9. *Cont.*

Figure A9. Linear regression of flight altitude above ground level in relation to temperature, (**a**–**d**) grouped by track type and for (**e**) all track types collectively. For each regression, the median flight altitude was used for each °C. The regression equation and correlation coefficient (r_s, *** $p < 0.001$) is given for each plot. The horizontal bars represent the variance around each median (IQR).

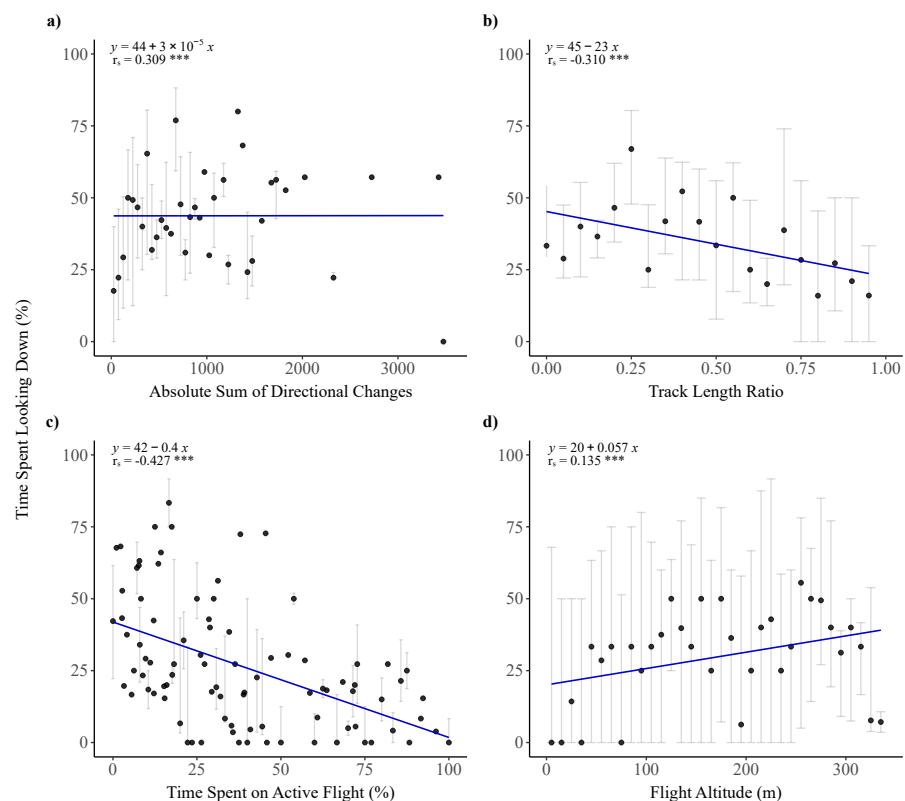*Appendix F.3. Flight Behavior in Relation to Vigilance*

Figure A10. Linear regression of flight vigilance quantified by % time each individual spent looking down in relation to (**a**) track symmetry (sum of directional changes), (**b**) track tortuosity (track length ratio), (**c**) proportion of time spent on active flight, and (**d**) flight altitude. For each regression, the median proportion of time spent looking down was used for each corresponding variable (every 50 sum of directional changes; each 0.05 ratio value; each % for active flight; and every 10 m). The regression equation and correlation coefficient (r_s, *** $p < 0.001$) is given for each plot. The horizontal bars represent the variance around each median (IQR).

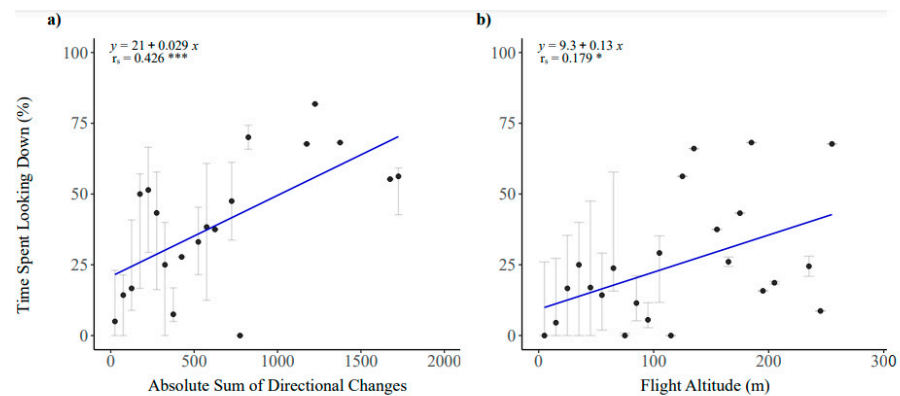*Appendix F.4. Flight Behavior of Birds in Active Flight*

Figure A11. Linear regression, for individuals in active flight, of the proportion of time each individual spent looking down in relation to (**a**) the sum of directional changes, and (**b**) flight altitude above ground level. For each regression, the median proportion of time spent looking down was used for each corresponding variable (every 200 sum of directional changes; and every 10 m for flight altitude). The regression equation and correlation coefficient (r_s, * $p < 0.05$, *** $p < 0.001$) is given for each plot. The horizontal bars represent the variance around each median (IQR).
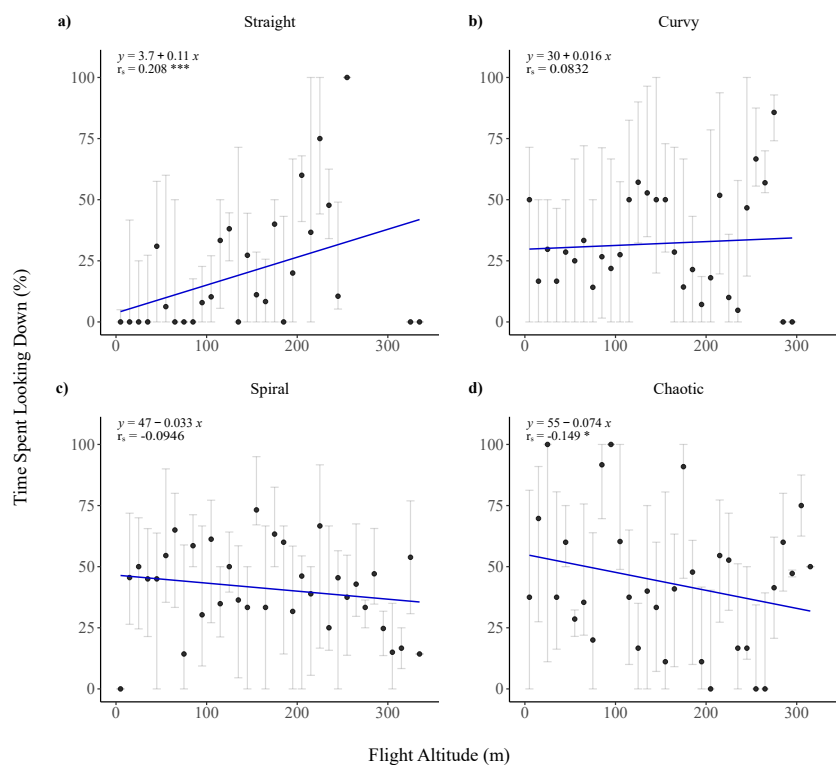
Appendix F.5. Vigilance

Figure A12. Linear regression of the proportion of time each individual spent looking down in relation to flight altitude above ground level for (**a**) straight tracks, (**b**) curvy tracks, (**c**) spiral tracks, and (**d**) chaotic tracks. For each regression, the median proportion of time spent looking down was used for every 10 m. The regression equation and correlation coefficient (r_s, * $p < 0.05$, *** $p < 0.001$) is given for each plot. The horizontal bars represent the variance around each median (IQR).
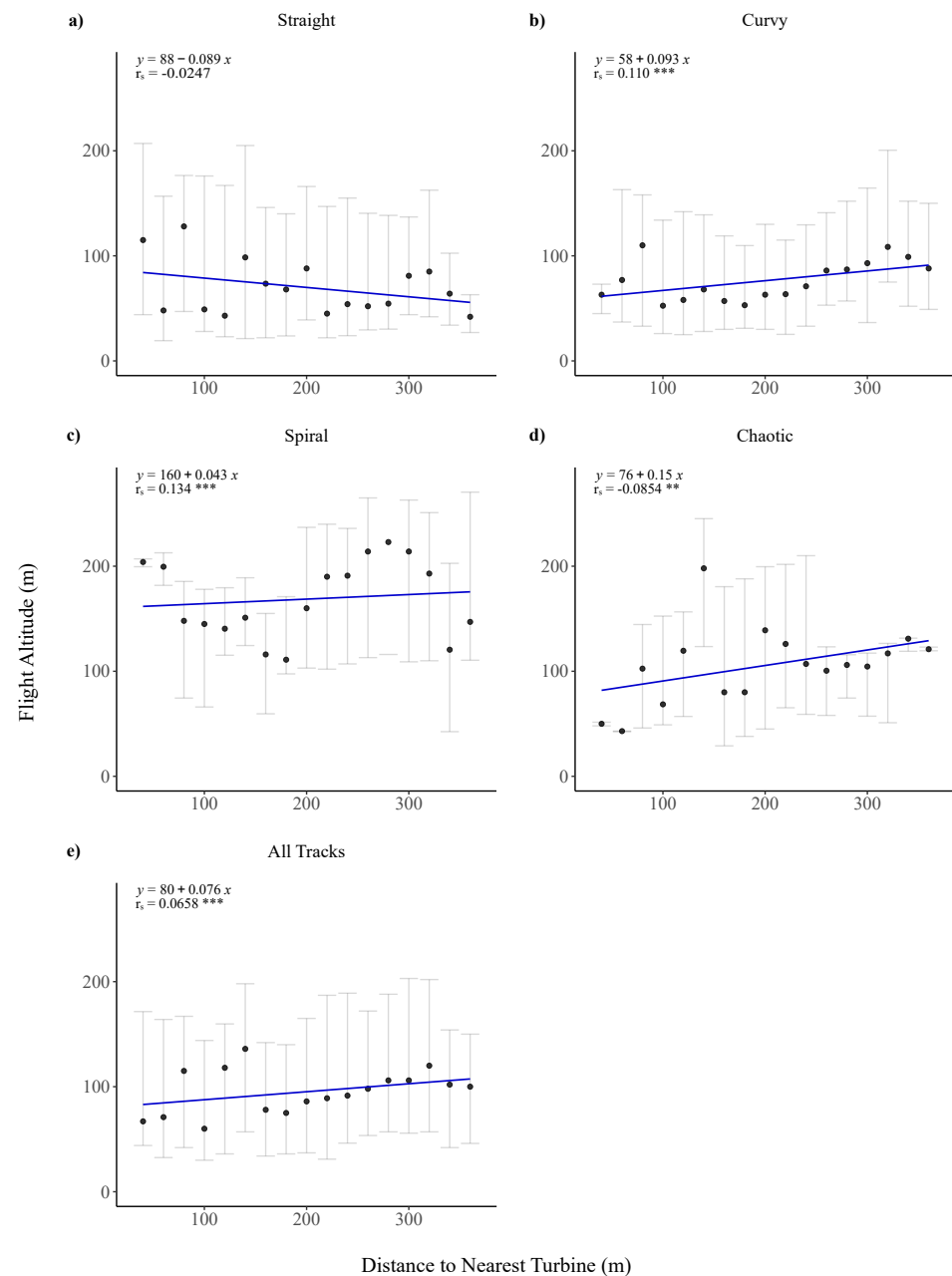
Appendix F.6. Avoidance Behavior

Figure A13. Linear regression of distance to the nearest turbine in relation to flight altitude above ground level, (**a**–**d**) grouped by track type and for (**e**) all track types collectively. For each regression, the median flight altitude was used for every 20 m. The regression equation and correlation coefficient (r_s, ** $p < 0.01$, *** $p < 0.001$) is given for each plot. The horizontal bars represent the variance around each median (IQR).

Appendix G. Model Selection

The automated model selection was carried out for models both with and without interactions for flight vigilance, flight altitude, track tortuosity, and track symmetry. For each response variable the models with and without interactions were compared based on their respective AIC values. Moreover, an ANOVA test using the χ^2 test statistic was also used to assess the goodness of fit of the nested regression models, i.e., the models with and without interactions [36]. The model with interactions was selected as the best model if the addition of interaction terms significantly increased the model's goodness of fit, if not the simpler of

the two models, i.e., the model without interactions, was selected. The models that were not selected as the best models are presented below.

Table A4. Details of the automated model selection completed with *glmulti*. The * annotation indicates that the addition of interaction terms significantly improved the model's goodness of fit.

| Name	No. of Covariates	No. of Generations	Best AIC
Flight vigilance *			
Without interactions	8	250	48.1
With interactions	8	490	36.3
Flight altitude *			
Without interactions	8	250	4000
With interactions	8	380	3982
Track tortuosity			
Without interactions	7	250	78.4
With interactions	7	500	70.7
Track symmetry *			
Without interactions	7	250	5419
With interactions	7	520	5400

Importance of Model Terms
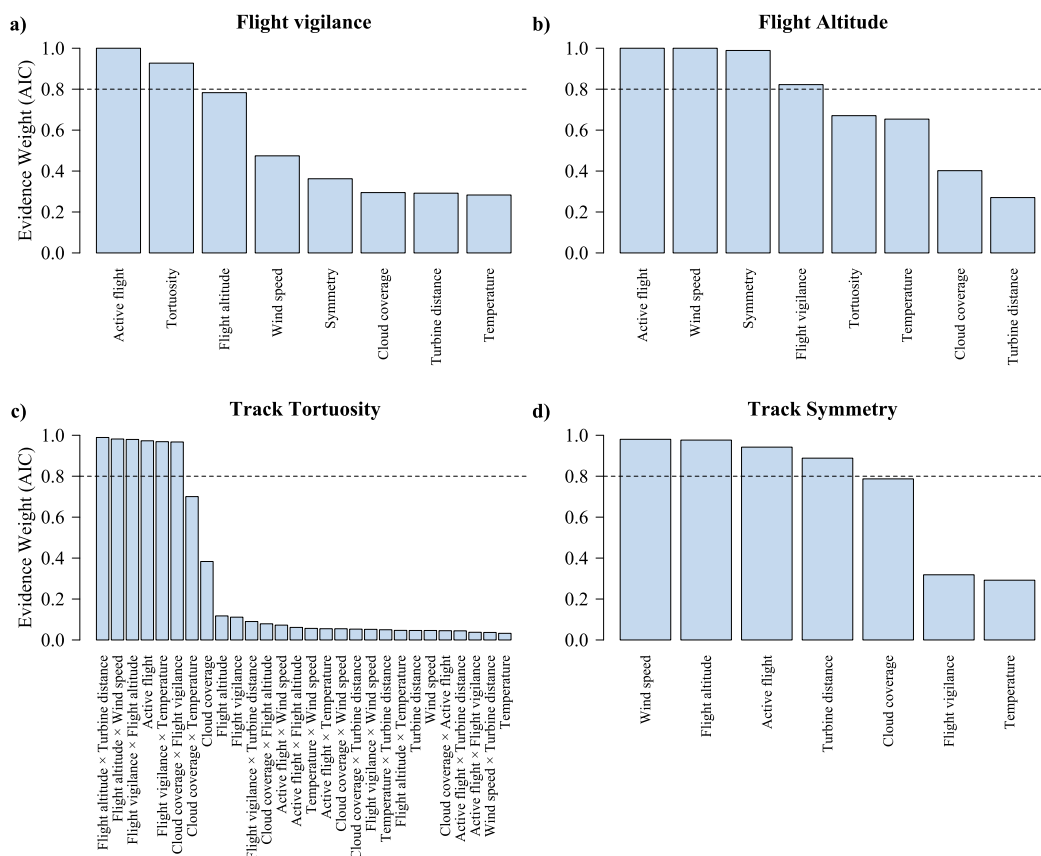
Figure A14. Relative importance of each model term when assessing (**a**) flight vigilance as the response variable without interactions, (**b**) flight altitude as the response variable without interactions, (**c**) track tortuosity as the response variable with interactions, and (**d**) track symmetry as the response variable without interactions. Each term's relative importance was estimated with the automated model selection as the sum of Akaike evidence weights of all models in which the term appears.

References

1. Drewitt, A.L.; Langston, R.H.W. Assessing the Impacts of Wind Farms on Birds. *IBIS* **2006**, *148*, 29–42. [CrossRef]
2. Madders, M.; Whitfield, D.P. Upland Raptors and the Assessment of Wind Farm Impacts. *IBIS* **2006**, *148*, 43–56. [CrossRef]
3. de Lucas, M.; Janss, G.F.E.; Whitfield, D.P.; Ferrer, M. Collision Fatality of Raptors in Wind Farms does not Depend on Raptor Abundance. *J. Appl. Ecol.* **2008**, *45*, 1695–1703. [CrossRef]
4. Smallwood, K.S.; Thelander, C. Bird Mortality in the Altamont Pass Wind Resource Area, California. *J. Wildl. Manag.* **2008**, *72*, 215–223. [CrossRef]
5. Bevanger, K.; Berntsen, F.; Clausen, S.; Dahl, E.L.; Flagstad, Ø.; Follestad, A.; Halley, D.; Hanssen, F.; Johnsen, L.; Kvaløy, P.; et al. *Pre- and Post-Construction Studies of Conflicts Between Birds and Wind Turbines in Coastal Norway (Bird-Wind)*; Report on Findings 2007–2010; Norwegian Institute for Nature Research: Trondheim, Norway, 2010.
6. Katzner, T.E.; Brandes, D.; Miller, T.; Lanzone, M.; Maisonneuve, C.; Tremblay, J.A.; Mulvihill, R.; Merovich , G.T., Jr. Topography Drives Migratory Flight Altitude of Golden Eagles: Implications for On-Shore Wind Energy Development. *J. Appl. Ecol.* **2012**, *49*, 1178–1186. [CrossRef]
7. Loss, S.R.; Will, T.; Marra, P.P. Estimates of Bird Collision Mortality at Wind Facilities in the Contiguous United States. *Biol. Conserv.* **2013**, *168*, 201–209. [CrossRef]
8. Marques, A.T.; Batalha, H.; Rodrigues, S.; Costa, H.; Pereira, M.J.R.; Fonseca, C.; Mascarenhas, M.; Bernardino, J. Understanding Bird Collisions at Wind Farms: An Updated Review on the Causes and Possible Mitigation Strategies. *Biol. Conserv.* **2014**, *179*, 40–52. [CrossRef]
9. Watson, R.T.; Kolar, P.S.; Ferrer, M.; Nygård, T.; Johnston, N.; Hunt, W.G.; Smit-Robinson, H.A.; Farmer, C.J.; Huso, M.; Katzner, T.E. Raptor Interactions with Wind Energy: Case Studies from Around the World. *J. Raptor Res.* **2018**, *52*, 1–18. [CrossRef]
10. Perold, V.; Ralston-Paton, S.; Ryan, P. On a Collision Course? The Large Diversity of Birds Killed by Wind Turbines in South Africa. *J. Afr. Ornithol.* **2020**, *91*, 228–239. [CrossRef]
11. Powlesland, R.G. Impacts of Wind Farms on Birds: A Review. *Sci. Conserv.* **2009**, *289*, 51.
12. Directorate-General for Environment (European Commision). Guidance Document: Wind Energy Development and Natura 2000. 2010. Available online: https://viuredelairebcn.cat/wp-content/uploads/2021/09/Wind-energy-developments-and-Natura-2000_resum.pdf (accessed on 30 August 2022).
13. May, R.; Hoel, P.L.; Langston, R.; Dahl, E.L.; Bevanger, K.; Reitan, O.; Nygård, T.; Pedersen, H.C.; Røskaft, E.; Stokke, B.G. *Collision Risk in White-Tailed Eagles. Modelling Collision Risk Using Vantage Point Observations in Smøla Wind-Power Plant*; Report 639; Norwegian Institute for Nature Research: Trondheim, Norway, 2010.
14. Garvin, J.C.; Jennelle, C.S.; Drake, D.; Grodsky, S.M. Response of Raptors to a Wind farm. *J. Appl. Ecol.* **2011**, *48*, 199–209. [CrossRef]
15. Barrios, L.; Rodríguez, A. Behavioural and Environmental Correlates of Soaring-bird Mortality at On-shore Wind Turbines. *J. Appl. Ecol.* **2004**, *41*, 72–81. [CrossRef]
16. Johnston, N.N.; Bradley, J.E.; Otter, K.A. Increased Flight Altitudes Among Migrating Golden Eagles Suggest Turbine Avoidance at a Rocky Mountain Wind Installation. *PLoS ONE* **2014**, *9*, e93030. [CrossRef]
17. Murgatroyd, M.; Photopoulou, T.; Underhill, L.G.; Bouten, W.; Amar, A. Where Eagles Soar: Fine-Resolution Tracking Reveals the Spatiotemporal Use of Differential Soaring Modes in a Large Raptor. *Ecol. Evol.* **2018**, *8*, 6788–6799. [CrossRef] [PubMed]
18. Marques, A.T.; Santos, C.D.; Hanssen, F.; Muñoz, A.; Onrubia, A.; Wikelski, M.; Moreira, F.; Palmeirim, J.M.; Silva, J.P. Wind Turbines Cause Functional Habitat Loss for Migratory Soaring Birds. *J. Anim. Ecol.* **2019**, *89*, 93–103. [CrossRef]
19. Dahl, E.L.; May, R.; Hoel, P.L.; Bevanger, K.; Pedersen, H.C.; Røskaft, E.; Stokke, B.G. White-Tailed Eagles (*Haliaeetus Albicilla*) Smøla Wind. Plant, Cent. Norway, Lack Behav. Flight Responses Wind Turbines. *Wildl. Soc. Bull.* **2013**, *37*, 66–74. [CrossRef]
20. Cook, A.S.C.P.; Humphreys, E.M.; Masden, E.A.; Burton, N.H.K. The Avoidance Rates of Collision Between Birds and Offshore Turbines-BTO Research Report No. 656. *Scott. Mar. Freshw. Sci.* **2014**, *5*.
21. Rydell, J.; Ottvall, R.; Pettersson, S.; Green, M. *Report 6791 The Effects of Wind Power on Birds and Bats*; Digitala Vetenskapliga Arkivet: Stockholm, Sweden, 2017.
22. Whitfield, D.P.; Madders, M. *Deriving Collision Avoidance Rates for Red Kites Milvus Milvus*; Natural Research Information Note 3; Natural Research Ltd.: Banchory, UK, 2006.
23. Cabrera-Cruz, S.A.; Villegas-Patraca, R. Response of Migrating Raptors to an Increasing Number of Wind Farms. *J. Appl. Ecol.* **2016**, *53*, 1667–1675. [CrossRef]
24. Mojica, E.K.; Watts, B.D.; Turrin, C.L. Utilization Probability Map for Migrating Bald Eagles in Northeastern North America: A Tool for Siting Wind Energy Facilities and Other Flight Hazards. *PLoS ONE* **2016**, *11*, e0157807. [CrossRef]
25. Smallwood, K.S.; Bell, D.A. Effects of Wind Turbine Curtailment on Bird and Bat Fatalities. *J. Wildl. Manag.* **2020**, *84*, 685–696. [CrossRef]
26. McClure, C.J.W.; Martinson, L.; Allison, T.D. Automated Monitoring for Birds in Flight: Proof of Concept with Eagles at a Wind Power Facility. *Biol. Conserv.* **2018**, *224*, 26–33. [CrossRef]
27. Esri; HERE; Garmin; FAO; NOAA; USGS. World Topographic Map. 2020. Available online: http://www.esri.com/ (accessed on 1 March 2021).
28. Wirdheim, A.; Corell, M. *Fågelrapport 2015*; Fågelåret 2015; BirdLife Sverige: Mörbylånga, Sweden, 2015.

29. Aldén, L.; Ottvall, R.; Soares, J.P.D.S.; Klein, J.; Liljenfeldt, J. *Rapport: Samexistens Örnar och Vindkraft på Gotland*; Digitala Vetenskapliga Arkivet: Stockholm, Sweden, 2017.

30. Jensen, B.B. Efterårets Rovfugletræk. *Fuglehåndbogen på Nettet* **2015**, *1*, 21122015.

31. Esri. *ArcGIS Pro 2.5.0*; Environmental Systems Research Institute: Redlands, CA, USA, 2020.

32. SMHI, Swedish Meteorological and Hydrological Institute. Norrköping, 2020. Available online: www.smhi.se (accessed on 30 August 2022).

33. R Core Team. *R: A Language and Environment for Statistical Computing*; R Foundation for Statistical Computing: Vienna, Austria, 2020.

34. Whitlock, M.C.; Schluter, D. *The Analysis of Biological Data*, 2nd ed.; W. H. Freeman and Company: New York, NY, USA, 2015.

35. Calcagno, V.; de Mazancourt, C. glmulti: An R Package for Easy Automated Model Selection with (Generalized) Linear Models. *J. Stat. Softw.* **2010**, *34*. [CrossRef]

36. Zuur, A.F.; Ieno, E.N.; Walker, N.J.; Saveliev, A.A.; Smith, G.M. *Mixed Effects Models and Extensions in Ecology with R*; Statistics for Biology and Health; Springer: New York, NY, USA, 2009.

37. Walker, A.; Mcgrady, M.; Mccluskie, A.; Madders, M.; Mcleod, D.R.A. Resident Golden Eagle Ranging Behaviour Before and After Construction of a Windfarm in Argyll. *Scott. Birds* **2005**, *25*, 24–40.

38. Miller, T.; Lockhart, M.; Braham, M.; Smith, B.; Katzner, T. *Flight Behavior of Golden Eagles in Wyoming: Implications for Wind Power*; Wind Wildlife Research Meeting; American Wind Wildlife Institute: Washington, DC, USA, 2020.

39. Bergen, S.; Huso, M.; Braham, M.; Duerr, A.; Katzner, T.; Miller, T.; Schmuecker, S. *Improved Behavioral Classification of Flight Behavior Informs Risk Modeling of Bald Eagles at Wind Facilities in Iowa*; Wind Wildlife Research Meeting; American Wind Wildlife Institute: Washington, DC, USA, 2020.

40. Kuehn, M.; Merrill, L.; Bloom, P.; Riley, E. *Temporal, Topographic, and Meteorological Correlates of Golden Eagle Flight Behavior in California's Tehachapi Wind Resource Area*; Wind Wildlife Research Meeting; American Wind Wildlife Institute: Washington, DC, USA, 2020.

41. Lanzone, M.J.; Miller, T.A.; Turk, P.; Brandes, D.; Halverson, C.; Maisonneuve, C.; Tremblay, J.; Cooper, J.; O'Malley, K.; Brooks, R.P.; et al. Flight Responses by a Migratory Soaring Raptor to Changing Meteorological Conditions. *Anim. Behav.* **2012**, *8*, 710–713. [CrossRef]

42. Wiggelinkhuizen, E.; den Boon, J. *Monitoring of Bird Collisions in Wind Farm Under Offshore-like Conditions Using WT-BIRD System*; Energy Research Centre of the Netherlands: Petten, The Netherlands, 2010.